

Switching in Orientation of Macromolecular Helical Rod Silicon on the Solid Surfaces

Masanobu Naito,* Naho Saeki, Michiya Fujiki,* and Akihiro Ohira

Graduate School of Materials Science, Nara Institute of Science and Technology, 8916-5, Takayama, Ikoma, Nara 630-0101, Japan, and CREST-JST, 4-1-8 Hon-Cho, Kawaguchi, Saitama 332-0012, Japan

Received September 1, 2006; Revised Manuscript Received November 23, 2006

ABSTRACT: The present paper reports the self-ordering behavior of rod-like and random-coiled poly-(dialkylsilane)s with Si–H termini on HO-presented substrates. The effects of stiffness and molecular length of poly(dialkylsilane)s and substrates were investigated by a combination of quartz crystal microbalance, specular reflectance UV spectroscopy, and atomic force microscopy. A simple immersion of the HO-presented substrates into poly(*n*-decylisobutylsilane) (PDBS)/isooctane enabled the manipulation of cooperative structural phase transition from horizontal to almost vertical orientation to the substrate. Furthermore, the orientation behavior of vertically self-assembled PDBS depended on its molecular weight. On the other hand, a random-coiled poly-(methyl-*n*-propylsilane) (PMPS) was only horizontally immobilized, resulting in the formation of a mushroom-like structure on HO-presented substrates. Knowledge gained from these studies may lead to a new, simple approach designed to fabricate vertically and/or horizontally self-assembled nanoarrays with rod-like and/or random-coiled semiconducting macromolecules onto solid surfaces.

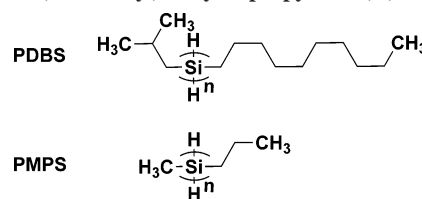
Introduction

The inherent nature of nonamphiphilic chain-like molecules at the solid–liquid interface has long been puzzling. The adsorption–desorption process and shapes of these molecules at the interface remain unclear due to the lack of proper model molecules with a broad range of molecular length (*L*) and detection systems with ultrahigh sensitivity and high accuracy. However, structural transition of amphiphilic molecules at the air–water/solid–liquid interface has been comprehensively understood experimentally and theoretically.^{1,2}

Among various chain-like molecules and macromolecules, semiflexible high polymers (SFPs) with a relatively long persistence length (*q*), exhibiting an intermediate manner between rigid rod and random coil, are currently attractive materials in polymer physics, surface topology science, self-assembled monolayers (SAM), polymer-to-electrode interconnections, molecular-based electronics, optoelectronics, and photonics.^{3–7} For example, SFPs with *L* < *q*, adopting an almost ideal rod structure, show several unique physical properties similar to lyotropic liquid crystals,^{8–11} thermotropic smectic and/or cholesteric liquid crystals,^{12,13} and highly delocalized excitons confined to a quasi-one-dimensional (Q1D) quantum wire.¹⁴ Most SFPs with *L* > *q* as well as most ordinary polymers, however, exhibit typical characteristics of random-coiled structures. Knowledge and understanding of SFPs on solid surfaces as functions of *L* and *q* are of particular importance in basic science and various applications.

To elucidate the invisible uniqueness of SFPs at the solid–liquid interface, we chose certain Si-based macromolecular Q1D, poly(*n*-decylisobutylsilane) (PDBS) with Si–H termini,¹⁵ ranging in *L* from ca. 4 nm to ca. 760 nm (Scheme 1). The value of *L* was estimated by the product of the number-averaged degree of polymerization and contour length of 7₃ helical structure of PDBS (0.185 nm). Less polar Si–H termini may effectively interact with functional groups of the solid surface with the help of trace amounts of water in solvent and/or at the interface.

Scheme 1. Chemical Structures of Poly(*n*-decylisobutylsilane) (PDBS) and Poly(methyl-*n*-propylsilane) (PMPS)



PDBS features a semiflexible rope-like structure with a relatively long *q* of 60 nm in isooctane at 20 °C, adopting an optically inactive main chain with an equal amount of *P*-7₃ and *M*-7₃ helices.¹⁶ For comparison, poly(methyl-*n*-propylsilane) (PMPS) with Si–H termini, which have a very short *q* of 1–2 nm and a broad main chain absorption at 305 nm, was tested as a random-coiled polysilane (Scheme 1).¹⁷

In a previous paper, we demonstrated chemical immobilization of Si–H-terminated PDBS with a sufficiently long *L* (ca. 760 nm) at the mica/isooctane and quartz/isooctane interfaces, by reacting the termini with a silanolic surface in the presence of triethylamine (NEt₃), confirming by ordinary UV absorption spectroscopy and atomic force microscopy (AFM).¹⁸ AFM observation successfully provided topological images of highly entangled PDBS on the mica surface, fully reflecting the random-coiled SFP with *L* > *q* in solution.

The present paper reports the first clear *L* and *q* dependency of critical changes in molecular orientation and molecular shapes of PDBS and PMPS at the isooctane/solid interfaces, where the gold surface used in this work was modified with alcoholic alkyl groups and the mica surface was naturally covered with silanolic groups. It was found that, when PDBS was *L* < *L*_{th} (threshold *L*) ~ *q*/4, cooperative transition in molecular orientation from horizontal to almost vertical alignment spontaneously occurred at the interface as a factor of immersion time of PDBS onto the solid. PDBS with *L* > *L*_{th} did not undergo such cooperativity at the interface. PMPS with *L* ≫ *q* formed mushroom-like structures at the mica surface.

* Corresponding authors. E-mail: mnaito@ms.naist.jp, fujikim@ms.naist.jp.

Experimental Section

Apparatus. FT-IR spectra were recorded on a Horiba model FT-730 (Kyoto, Japan) with a TGS detector at room temperature. Specular reflectance UV (SR-UV) spectra on an Au-coated surface were measured by a JASCO V-570 spectrophotometer (Tokyo, Japan) and transformed to UV absorption and refractive index terms by Kramers–Kronig (K–K) analysis (JASCO, built-in program of V-570).

The absolute number-average molecular weight (M_n) and polydispersity index (PDI) of PDBS and PMPS were determined by gel permeation chromatography (GPC) with a Shimadzu model A-103 (Kyoto, Japan) (eluent: tetrahydrofuran; flow rate: 1.0 mL/min; and column temperature: 40 °C) equipped with a Polymer Laboratories PLgel Mixed-B (Worcester, MA) (300 mm in length, 7.5 mm in diameter), a Shimadzu RID-10A (Kyoto, Japan) refractive index detector, and a Viscotek model T60A triple detector (Houston, TX) consisting of a right-angle laser light scattering detector (RALLS) (λ_0 : 670 nm) and a four-capillary differential viscometer. The results were analyzed using worm-like cylinder theory (Viscotek, built-in program).

Observation by atomic force microscopy (AFM) in dynamic force mode was conducted using a Seiko Instruments (SII) model SPA-3800N microscope with an SPA 400 scanner (Tokyo, Japan) equipped with Si-DF-20 tips at ambient condition. Drive frequencies of the cantilevers were typically set at 110–150 kHz, and images were collected at the maximum available pixel number (512).

A 9 MHz quartz crystal microbalance was measured with a U.S.I. System model Q-200E (Fukuoka, Japan). A 1.0 Hz frequency decrease on 9 MHz QCM was calculated to be equivalent to a 6.2 ng cm⁻² mass increase on Au electrodes.

Frequency changes were monitored by a Hewlett-Packard universal counter model 53131A (Colorado). Au electrodes (4.0 mm in diameter, 12.6 mm² in area) were made on both sides of an AT-cut quartz crystal plate (8.0 mm in diameter). The Au electrodes were cleaned with piranha solution (4:1, v/v 96% H₂SO₄/30% H₂O₂) for 15 min and washed with Milli-Q water to eliminate organic contamination before measurement. This process was repeated twice. **Caution:** The piranha solution is a highly corrosive agent, and appropriate safety precautions should be taken, including the use of acid-resistant gloves and adequate shielding.

Sample Preparation. The Si–H termini containing PDBS samples with desired L and narrow PDI were prepared by condensating the corresponding dichlorosilane with sodium in hot toluene at 120 °C in the presence of 18-crown-6 (2 mol % to the monomer) and were isolated by fractional precipitation with careful successive additions of 2-propanol, EtOH, and MeOH. Details of the synthesis are already described in previous papers.^{19,20} Si–H termini, which were confirmed by FT-IR spectroscopy with Si–H stretching in the region around 2100 cm⁻¹, were spontaneously introduced by abstracting hydrogen from solvent and/or crown ether during polymerization.¹⁵ We also carefully confirmed by GPC-RALLS that the PDBS did not change its molecular weight (corresponding to L) and by UV/FT-IR spectroscopies that the Si main chain of PDBS did not transform to siloxane. The values of M_n and PDI of PDBS and PMPS used are summarized in Tables 1 and 2, respectively. The values of L of PDBS and PMPS were given by 0.185 n . Here, 0.185 and n are values of the Si–Si projection length in nanometers and the degree of polymerization, respectively.

For the real-time QCM measurements, Au QCM electrodes with SAM of 6-mercapto-1-hexanol (Aldrich) were used as an alcoholic (HO–C₆H₁₂S–) substrate, immersed in a 1.0 × 10⁻² M isooctane solution of PDBS for 25 h, followed by washing with fresh isooctane for 30 min and subsequent drying with a gentle N₂ stream to eliminate physically adsorbed PDBS. A small amount of NEt₃ (0.16% w/w in isooctane) was added to effectively react the Si–H termini with HO groups on the SAM surface, as previously reported.¹⁸

Effects of immersion time on change in morphology of the PDBS and PMPS were directly observed by an AFM on freshly cleaved mica (as an alternative to the HO-pretreated Au surface). The mica

Table 1. Characterization of Poly(*n*-decylisobutylsilane) (PDBS)

entry	$M_n^a \times 10^4$	L^b	PDI ^c	$\epsilon^d \times 10^4$	λ_{max}^e
1	0.5	4.1	1.83	3.8	318
2	0.6	5.1	1.90	3.8	319
3	0.9	7.0	1.80	4.0	320
4	1.1	8.6	1.14	4.1	320
5	1.3	10.9	1.90	4.3	320
6	2.0	16.2	1.70	4.5	320
7	2.2	18.2	2.00	4.6	320
8	3.0	24.8	2.50	4.6	320
9	4.9	40.0	2.10	4.6	320
10	12.2	100.0	2.50	4.6	320
11	41.4	339.1	2.70	4.7	320
12	55.1	450.9	2.55	4.9	320
13	93.2	763.0	1.95	4.9	320

^a M_n = number-average molecular weight. ^b L = molecular length/nm. ^c PDI = polydispersity index (M_w/M_n). ^d ϵ = Molar absorption coefficient/(Si repeat unit)⁻¹ dm³ cm⁻¹. ^e λ_{max} = maximum absorption wavelength/nm.

Table 2. Characterization of Poly(methyl-*n*-propylsilane) (PMPS)

entry	$M_n^a \times 10^3$	L^b	PDI ^c	$\epsilon^d \times 10^3$	λ_{max}^e
1	3.8	8.0	1.11	5.0	305

were immersed in 10.0 mM isooctane solution of PDBS (L = 8.6 nm (< L_{th}) and PDI = 1.14) (abbreviated to PDBS-8.6) or PMPS (L = 8.0 nm and PDI = 1.11) (abbreviated to PMPS-8.0) for a range of immersion times and washed with fresh isooctane for 30 min to eliminate organic contamination and physically adsorbed PDBS-8.6 or PMPS-8.0 on the surface. Successively, the PDBS or PMPS immobilized on mica was dried under a gentle N₂ stream.

Analysis. Freshly prepared PDBS or PMPS on the QCM surfaces was characterized by a combination of QCM and SR-UV spectroscopy at an incident angle of 5°. QCM was able to monitor the change in mass on the QCM surface at the nanogram level. Maximum occupied molecular area (A_{max}) was calculated from the mass change on the QCM substrate, as follows:

$$\text{occupied molecular area } (A_{max}) \text{ (nm}^2 \text{ molecule}^{-1}) = \frac{m_{\text{molecule}} (\text{g molecule}^{-1})}{10^{-14} \Delta m' \text{ (ng nm}^{-2})} \quad (1)$$

where m_{molecule} is number-average molecular weight per PDBS or PMPS single chain calculated by GPC-RALLS.

From QCM analysis, $\Delta m'$ (ng nm⁻²) was derived from Δm (ng cm⁻²) of the increased mass on the Au electrode.

SR-UV spectra on the Au electrodes were measured. Obtained SR-UV spectra were transformed to UV absorption and refractive index terms by K–K analysis. The absorption term provides information about the orientation of PDBS and PMPS on the surface because the polysilanes have a highly anisotropic UV absorption around 280–340 nm with an intense molar absorbance coefficient, e.g., ϵ (PDBS): 40 000–50 000/(Si repeat unit)⁻¹ dm³ cm⁻¹ (at 320 nm in isooctane at 25 °C); ϵ (PMPS): 5000–6500/(Si repeat unit)⁻¹ dm³ cm⁻¹ (at 305 nm in isooctane at 25 °C), assigned to the lowest Si σ –Si σ^* transition parallel to the Si main chain axis only (not perpendicular).

Results and Discussion

Figure 1 shows the double-logarithmic plots of A_{max} against L (a dotted line indicates the q value of PDBS). With an increase in L , a drastic change in A_{max} values was observed with a threshold L_{th} of ca. 15 nm. In the region of $L > L_{th}$, the values of A_{max} increased almost linearly with increases in L , reflecting the typical random-coiled nature of SFP in solution. On the contrary, for the region of $L < L_{th}$, the values of A_{max} were almost independent of the L values at a constant value of ca. 2.0 nm²/molecule. The latter result led to the idea that PDBS can adopt an almost ideal rigid rod and may form a vertically

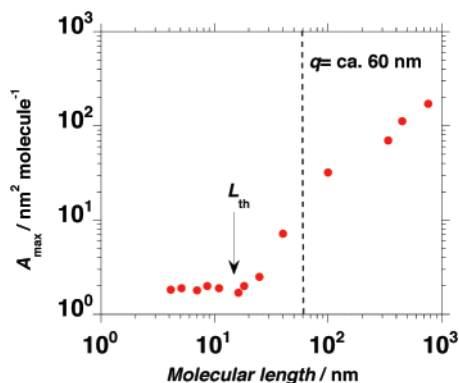


Figure 1. Molecular length (L) dependency of PDBS at the alcoholic Au QCM/isooctane interface on the value of A_{\max} ; [PDBS] = 1.0×10^{-2} M. Dotted line: persistence length q (60 nm: PDBS in isooctane at 25 °C).¹⁶

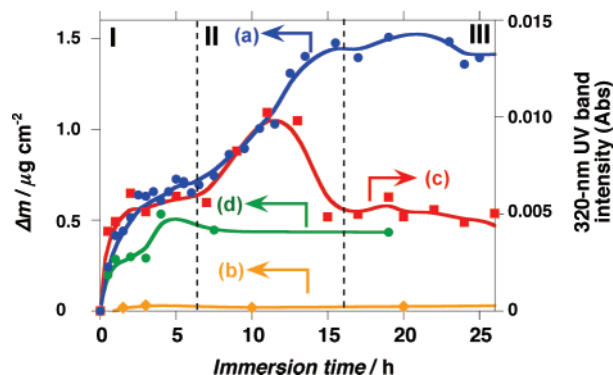


Figure 2. Changes in QCM mass (Δm) of PDBS-8.6 ($L = 8.6$ nm) with immersion time at the (a) isooctane/alcoholic and (b) isooctane/nonalcoholic Au QCM interfaces. (c) Changes in the 320 nm UV band intensity of the PDBS-8.6 (Abs) at the isooctane/alcoholic Au QCM interface. (d) Changes in the Δm value of PMPS-8.0 ($L = 8.0$ nm) with immersion time at the isooctane/alcoholic Au QCM interface.

oriented, close-packed single PDBS layer on the surface due to a sufficiently shorter L than q . Indeed, the given A_{\max} values of PDBS with $L < L_{th}$ are almost equal to that of optically active, semiflexible poly(*n*-decyl-(*S*)-methylbutylsilane) with a P -7₃ helix and a long q of 70 nm in isooctane, ca. $1.8 \text{ nm}^2/\text{molecule}$ in a thermotropic liquid crystalline S_mA phase.¹³

To elucidate the temporal behavior of the adsorption–desorption process at the interface, we conducted QCM and SR-UV measurements of PDBS-8.6 with an immersion time of the Au electrode into its isooctane solution. It is evident that, as immersion time increases, the curve of the increase in the mass of PDBS-8.6 (Δm) by the QCM experiment did not trace the corresponding curve of change at 320 nm band intensity by the SR-UV experiment (see Figure 2). The QCM experiment clearly showed that dual plateaus exist, one each at immersion times of approximately 7 and 16 h (see Figure 2a, blue solid curve) and the amount of PDBS at the interface saturates at a constant value of ca. 1.4 g cm^{-2} , indicating plural types of adsorptions at the interface when immersion times exceeded 20 h. On the other hand, the SR-UV experiment showed more complex changes at the 320 nm band intensity with immersion times of ca. 7, 11, and 17 h (see Figure 2c, red solid curve), indicating the existence of plural adsorptions at the interface. To interpret these temporal behaviors in the QCM and SR-UV experiments, we classified the adsorption behaviors into three regions I, II, and III.

In region I, both the values of Δm and 320 nm band intensity steeply increased in a similar manner and almost reached the

first plateau, 0.7 g cm^{-2} and 0.7×10^{-2} , respectively, implicating a horizontal adsorption of PDBS main chains at the interface. In region II, Δm values gradually increased with immersion time from 7 to 17 h and reached the second equilibrium of 1.4 g cm^{-2} , whereas the values of the 320 nm band intensity gradually increased to ca. 1.0×10^{-2} at an immersion time of 11 h but abruptly decreased to ca. 0.5×10^{-2} from 11 to 17 h. Eventually, in region III, both values of Δm and 320 nm band intensity remained unchanged and reached the second equilibrium, $1.4 \mu\text{g cm}^{-2}$ and 0.5×10^{-2} , respectively.

For comparison, Δm of PMPS-8.0 reached a single plateau of $0.45 \mu\text{g cm}^{-2}$, when immersion time exceeded 3–4 h. Successive immersion of PMPS-8.0 did not induce any additional change in Δm value, suggesting no further adsorption at the interface (see Figure 2d, green solid curve).

To prove the idea that an interaction between the Si–H termini of PDBS and the HO groups at the Au QCM electrode is responsible for the temporal adsorption properties of PDBS, we achieved the same QCM and SR-UV experiments of PDBS-8.6 using a nonalcoholic ($\text{C}_{10}\text{H}_{21}\text{S}$) Au QCM electrode treated with 1-mercaptodecane (Wako). Indeed, PDBS was not adsorbed on the nonalcoholic Au electrode, indicating that the unique adsorption manner of PDBS-8.6 is induced only by a spontaneous, selective attractive interaction (not physical) between the Si–H termini of PDBS and the alcoholic groups of the surface (Figure 2b, orange solid curve). The presence of NEt_3 may effectively activate this interaction. The Si–H group of PDBS presumably turns to a Si–OH group by NEt_3 and a trace amount of water in isooctane. Interaction between the Si–OH group and alcoholic groups of the Au electrode may be responsible for the present unique adsorption.

To explain the origin of the marked decrease at the 320 nm band intensity with the concomitant increase in QCM mass in region II, we suggest that PDBS with $L < L_{th}$ at the interface spontaneously undergoes switching in the main chain orientation from horizontal to vertical. If PDBS is oriented vertically at the interface, the 320 nm UV band of PDBS could not be detected by SR-UV due to anisotropic transition moments along the Si main chain axis of the PDBS. Therefore, significant decrease in mass originated from the switching in orientation of PDBS from horizontal to almost vertical must occur. To explain the increase in the mass of QCM in region II, we propose that vertically oriented PDBS portions in the horizontally oriented PDBS array may provide an additional free lateral space at the interface, enabling a more densely packed, vertically oriented S_mA -like structure. The marked difference in the adsorption manner between PDBS-8.6 and PMPS-8.0 may suggest that the difference in rigidity of the polysilanes is responsible for the switch in orientation, rather than differences in L .

Direct molecular images of PDBS-8.6 on mica by AFM observation proved the hypothesis of orientation switching (see Figure 3). The key process of switching was attributed to an unexpected, unusual nucleation of almost vertically oriented PDBS domains spontaneously formed at the mica/isooctane interface when immersion reached a threshold time of 24 min. This unique nucleation of rod molecules onto the solid surface with time has not been reported theoretically or experimentally.

At an immersion time of 5 min, PDBS-8.6 formed sea-island-like domains with 0.8 nm in height (see Figure 3a). Since this value almost corresponds to the diameter of PDBS-8.6 main chain under dry conditions, the island domain might be made of PDBS-8.6 SAM with horizontal adsorption. With a prolonged

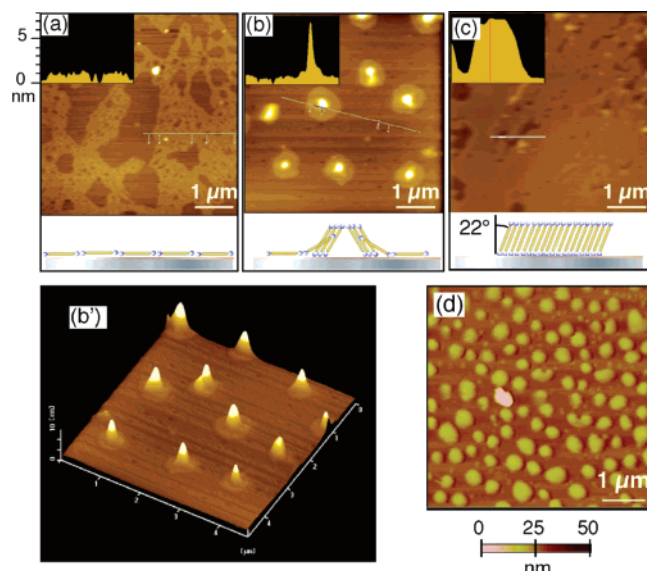


Figure 3. AFM images of PDBS-8.6 on mica at immersion times of (a) 5 min, (b) 24 min, and (c) 1 h. (b') 3D image of (b). (d) AFM image of PMPS-8.0 on mica at immersion time of 1 h.

immersion time, the island-like domains covered the entire mica surface. The horizontally aligned PDBS-8.6 flat film with a sea-island domain structure thus corresponds to region I of Figure 2.

When immersion time was 24 min, domain morphology abruptly changed (see Figure 3b,b'). The film turned to a "sunny-side-up"-like structure, consisting of two distinct cross-sectional heights of 2.0 and 8.0 nm, formed in the PDBS-8.6 nm flat film. The 8.0 nm part corresponds to the projection length of almost vertically oriented PDBS-8.6 with a tilt angle of 22° . The middle 2.0 nm part can be regarded as a snapshot of the transition state in the molecular orientation from horizontal to vertical. This "sunny-side-up"-like structure might be responsible for the uniqueness of the QCM and SR-UV data which appeared in region II of Figure 2. Eventually, at an immersion of 1 h, the entire area was covered with an almost uniform 8.0 nm film (see Figure 3c), indicating the formation of a nearly vertically aligned PDBS-8.6 with a tilt angle of 22° . On the other hand, PMPS-8.0 was not involved in orientation switching, but formed mushroom-like structures, even though the same immersion process as that of PDBS-8.6 was performed (Figure 3d). This may have originated from the random-coiled nature of PMPS-8.0 because, as far as possible, random-coiled polysilane avoid contact with poor solvents and form dot-like structures. In this case, the air could act as a poor solvent for the polysilanes. Thus, both termini of PMPS-8.0 could easily be immobilized on the surface, followed by formation of dot-like domains. Indeed, similar dot-like structures made by end-grafted single molecules of random coiled polysilanes have been reported.²¹ Considering the molecular length of PMPS-8.0, the dot-like structures of PMPS-8.0 may consist of several PMPS chains. Although tethered PMPS-8.0 swells in solution, during successive alternate immersion and dry processes, PMPS can interwind with the tethered PMPS domains, following enlargement of the dot-like structures with certain spaces between each domain.

It should be noted that vertically aligned PDBS film at the mica/isooctane interface forms ~ 25 times faster than at the alcoholic SAM-treated Au/isooctane interface. We assumed that hydrogen bonds between the Si-H (and/or Si-OH) termini of PDBS and silanolic groups of the solid formed more effectively than those between the Si-H (and/or Si-OH) termini and the

alcoholic groups of the SAM-treated Au. The higher rate may also be influenced by a small amount of bound water on the mica surface.

A recent study on the tethering nature of a random-coiled telechelic polymer at the surface by Monte Carlo simulation demonstrated alterations in the molecular shape from loosely packed "polymer mushrooms" with relaxed random-coiled structure to densely packed "polymer brushes" with extended rod-like forms, induced by nucleation of vertically aligned polymers at the surface.^{22,23} Although the space-temporal adsorption behavior of PDBS at the solid/isooctane interfaces is significantly different from the simulation, the key to these alterations may be almost identical: the number of hard rods in the domains at extraordinary high surface density spontaneously induces cooperative structural transitions from loosely to densely packed states. The sum of attractive interactions between the Si-H (and/or Si-OH) groups of PDBS and the alcoholic OH (or Si-OH) groups of the solid surfaces may effectively lead to vertically oriented PDBS SAM at the solid-liquid interface.

The present knowledge and understanding should provide information in designing and fabricating nanometer-scale electronic and optical devices using such Q1D rods as metal, metal oxide, carbon nanotube, and DNA.

Conclusion

QCM, SR-UV, and AFM experiments of semiflexible PDBS ranging in L from 4 to 760 nm and q of 60 nm showed that PDBS with $L = 8.6$ nm ($\ll q$) at the isooctane-alcoholic/silanolic solid interfaces with a critical immersion time spontaneously undergoes switching in main chain orientation from horizontal to almost vertical relative to the interfaces, reflecting its ideal rigid-rod nature.

Acknowledgment. M.N. thanks Ian Smith and Robert Wright for reading the entire text in its original form, Tomofumi Kubota for technical support, and Dr. Kento Okoshi for fruitful discussions. M.N. and M.F. acknowledge support by the Grant-in-Aids for Scientific Research (17750110 and 16205017), respectively. M.N. and M.F. also acknowledge partial funding from Scientific Research of Priority Areas (446) and the Grant-in-Aids for Scientific Research (16655046).

References and Notes

- (1) Gareth, R. *Langmuir-Blodgett Films*; Plenum Press: New York, 1990.
- (2) Ulman, A. *Chem. Rev.* **1996**, *96*, 1533–1554.
- (3) Moya, S. E.; Brown, A. A.; Azzaroni, O.; Huck, W. T. S. *Macromol. Rapid Commun.* **2005**, *26*, 1117–1121.
- (4) Samori, P.; Müllen, K.; Rabe, J. P. *Adv. Mater.* **2004**, *16*, 1761–1765.
- (5) Samori, P.; Donners, J. J. J. M.; Severin, N.; Otten, M. B. J.; Rabe, J. P.; Nolte, R. J. M.; Sommerdijk, N. A. J. M. *Langmuir* **2004**, *20*, 8955–8957.
- (6) Teramoto, A. *Prog. Polym. Sci.* **2001**, *26*, 667–720.
- (7) Siegmer, R.; David, C. *One-dimensional Metals: Conjugated Polymers, Organic Crystals, Carbon Nanotubes*, 2nd ed.; Wiley-VCH: Weinheim, 2004.
- (8) Yu, S. M.; Conticello, V. P.; Zhang, G.; Kayser, C.; Fournier, M. J.; Mason, T. L.; Tirrell, D. A. *Nature (London)* **1997**, *389*, 167–170.
- (9) Livolant, F.; Levelut, A. M.; Doucet, J.; Benoit, J. P. *Nature (London)* **1989**, *339*, 724–726.
- (10) Strzelecka, T. E.; Davidson, M. W.; Rill, R. L. *Nature (London)* **1988**, *331*, 457–460.
- (11) Oldenbourg, R.; Wen, X.; Meyer, R. B.; Caspar, D. L. D. *Phys. Rev. Lett.* **1988**, *61*, 1851–1854.
- (12) Asuke, T.; West, R. *Macromolecules* **1991**, *24*, 343–344.
- (13) Okoshi, K.; Kamee, H.; Suzuki, G.; Tokita, M.; Fujiki, M.; Watanabe, J. *Macromolecules* **2002**, *35*, 4556–4559.

- (14) Ichikawa, T.; Yamada, Y.; Kumagai, J.; Fujiki, M. *Chem. Phys. Lett.* **1999**, *306*, 275–279.
- (15) Saxena, A.; Okoshi, K.; Fujiki, M.; Naito, M.; Guo, G.-Q.; Hagihara, T.; Ishikawa, M. *Macromolecules* **2004**, *37*, 367–370.
- (16) Matsushima, S.; Yoshiba, K.; Teramoto, A.; Nakamura, N.; Sato, T.; Terao, K.; Fujiki, M. *Polym. Prepr. Jpn.* **2002**, *51*, 1820 [in Japanese].
- (17) Fujiki, M. *J. Am. Chem. Soc.* **1996**, *118*, 7424–7425.
- (18) Guo, G.-Q.; Naito, M.; Fujiki, M.; Saxena, A.; Okoshi, K.; Yang, Y.; Ishikawa, M.; Hagihara, T. *Chem. Commun.* **2004**, 276–277.
- (19) Miller, R. D.; Michl, J. *Chem. Rev.* **1989**, *89*, 1359–1410.
- (20) Fujiki, M. *J. Am. Chem. Soc.* **1994**, *116*, 11976–11981.
- (21) Furukawa, K. *Acc. Chem. Res.* **2003**, *36*, 102–110.
- (22) Penn, L. S.; Huang, H.-Q.; Sindkhedkar, M. D.; Rankin, S. E.; Chittenden, K.; Quirk, R. P.; Mathers, R. T.; Lee, Y. *Macromolecules* **2002**, *35*, 7054–7066.
- (23) Huang, H.-Q.; Rankin, S. E.; Penn, L. S.; Quirk, R. P.; Cheong, T. H. *Langmuir* **2004**, *20*, 5770–5775.

MA062019D